RDU151412

MICROSTRUCTURE AND MECHANICAL CHARACTERIZATION OF SEMISOLID METAL COMPONENTS FOR WROUGHT ALUMINIUM ALLOYS

(GAMBARAN SIFAT STRUKTUR KECIL DAN MEKANIKAL BAGI KOMPONEN LOGAM SEPARUH PEPEJAL ALOI TEMPAAN ALUMINIUM)

IR DR ASNUL HADI BIN AHMAD

PROF MADYA DR MAHADZIR BIN ISHAK@MUHAMMAD

IR DR MOHD RASHIDI BIN MAAROF

DR FADHLUR RAHMAN BIN ROMLEY

DR ZAKRI BIN GHAZALI

EN LUQMAN HAKIM BIN AHMAD SHAH

RESEARCH VOTES NO:

RDU 151412

RAGS 2015-1

FAKULTI KEJURUTERAAN MEKANIKAL

UNIVERSITI MALAYSIA PAHANG

2018

ACKNOWLEDGEMENTS

First and foremost, I would like to thank my research fellow which have supports both consciously and unconsciously with their knowledge in order to ensure this research can be completed. I appreciate all their contributions of time, ideas, knowledge, advice, guidance to make this research experience productive and stimulating. The joy and enthusiasm they have for their research was contagious and motivational for me, even during tough times in this research works. I am also thankful for the excellent example, they have provided as a successful researcher.

I would also grateful to all other researcher and industrial expertise for their help especially in materials characterization and experimental set-up. Special thanks also to UMP's Research and Innovation Department for their help in administrative works along this time.

ABSTRACT

This research present the works on the behaviour of wrought aluminium alloy via semisolid metal processing. Proper setting of pouring temperature and holding times is one of the important factors to obtain better microstructure formation and mechanical properties. In this work, thermal analysis experiments were conducted in order to obtain thermal profile of wrought aluminium alloy. This thermal analysis results such as liquidus, eutectic and solidus temperatures then were used as input parameters for subsequence experiments. In Direct thermal method (DTM) experiments, molten aluminium alloy was poured into copper tube moulds and cooled down to the semi-solid temperature before quenched in water at room temperature. The parameters of pouring temperature and holding times used were at 685 ℃, 665 ℃, 64 5℃ and 60 s, 40 s and 20 s respectively. The parameters used in DTM were purposely to study the effect on metallography and mechanical properties of aluminium alloy. Experimental results have proven that the solidified microstructure shown that, microstructure with smaller grain size has better hardness strength compared to bigger grain size. These results were represented with sample that processed with longer the holding time produced smaller grain size. The metallography analysis results was also found that the smallest microstructure formation and the hardest among samples was achieved at the sample with pouring temperature at 645 ℃ and holding time at 60 s. Result obtained from this research is very useful in order to understand aluminium behaviour which processed via semisolid metal processing route.

ABSTRAK

Kajian ini membentangkan kerja-kerja yang dijalankan ke atas gambaran sifat aloi aluminium tempaan menggunakan proses logam separuh pepejal. Penyelarasan suhu dan masa pegangan yang betul adalah salah satu faktor yang penting bagi menghasilkan struktur kecil dan kekuatan mekanikal bahan yang baik. Dalam kajian kerja ini, eksperimen analisis termal telah di jalankan bagi memperoleh sifat thermal bagi aloi aluminum tempaan. Hasil dapatan dari analisis termal ini seperti suhu cair, eutektik dan pejal seterusnya di gunakan sebagai parameter masukkan bagi experiment seterusnya. Di dalam experimen Kaedah Thermal Terus, aloi aluminium cair di curahkan ke dalam acuan tiub tembaga dan disejukkan ke aras suhu separuh pepejal sebelum ianya di lindap kejut ke dalam air bersuhu bilik. Suhu tuangan dan masa pegangan yang di gunakan masing-masing adalah pada 685 ℃, 665 ℃, 645℃ dan 60 s, 40 s, 20 s. Parameter yang di gunakan dalam experimen Kaedah Thermal Terus ini adalah bertujuan untuk mengkaji struktur kecil bahan dan sifat kekuatan mekanikal aloi aluminum. Hasil dapatan ekperimen telah membuktikan bahawa, struktur kecil bahan yang bersaiz lebih kecil menghasilkan kekuatan yang lebih baik dari struktur kecil bahan yang bersaiz besar. Hasil dapatan ini di di dapati dari sampel yang di proses dengan masa pegangan yang lebih lama. Hasil dapatan dari analisis struktur kecil bahan mendapati bahawa struktur bahan bersaiz paling kecil di perolehi dari sampel yang di proses menggunakan suhu tuangan 645 ℃ dan masa pegangan 60 s. Hasil dapatan dari kajian ini amat berguna untuk memastikan pemahaman yang lebih luas mengenai sifat-sifat aloi alumium yang di proses menggunakan cara pemprosesan logam separuh pepejal.

TABLE OF CONTENTS

CHAPTER 1

INTRODUCTION

1.1 EXECUTIVE SUMMARY

The use of the lightweight material such as aluminium alloy becomes one of the most important engineering materials in automotive and aerospace industries. Most of the automotive components such as cylinder heads, pistons, intake manifolds and chassis application in automotive power trains are made from aluminium alloy, typically by using a conventional metal casting process. The rapid growth in automotive industries in Malaysia, make the foundry a vital technology to keep Malaysia automotive sector can a head of the competition. There are several potential drawbacks are associated with conventional casting process, for instance shrinkage porosity formation, gas entrapment and hot cracking which leads to product rejection. Nevertheless, some of these conventional casting process weaknesses can be overcome by applying a semisolid metal (SSM) processing technique.

The main objective of this research is to evaluate the behaviour of wrought aluminium alloy by using SSM processing technique. In particular, this research objective is also to investigate the relationship between aluminium formed component quality and their mechanical properties. Initially, thermal analysis (TA) experiment will be conducted to determine suitable processing condition and understand the relationship between fraction solid and temperature. Different cooling medium will be used to replicate different cooling rate condition. The information gained from TA will be used to produce globular microstructure feedstock billet suitable for semisolid metal processing by direct thermal method. The quality of feedstock billet will be evaluated by using a forming die. The formed component microstructure and their mechanical properties then will be evaluated. The findings of this research will establish the detail material characteristic and behaviour of wrought aluminium alloy which was produced from a SSM processing technique. Such material characteristic and behaviour are vital information in order to enhance the formability and quality of low fluidity alloys such as wrought aluminium.

1.2 PROBLEM STATEMENT

There is interest to process wrought aluminium alloy within the semi-solid state due to the enhanced properties available from this alloy compared to its cast alloy alternatives. The properties of wrought aluminium alloy are superior to conventional cast alloy. Wrought aluminium alloy however is more difficult to process within the semi-solid state due to its narrow solidification range and higher propensity for hot tearing. Although extensive research within the literature has been carried out on wrought aluminium alloy, less attention was given to detailed experimental investigation on thermal profiles and microstructure at various solidification rates. There is also currently a lack of detailed experimental investigation within the literature into the thermal profiles for wrought aluminium alloy at various solidification rates which may occur during thixoforming. Furthermore, there has been a lack of information on the mechanical properties of wrought aluminium DTM feedstock billets which produced by thixoforming. Therefore, in order to gain detail material behaviour information for semisolid metal wrought aluminium alloy components, metallurgical and mechanical characterization works need to be conducted.

1.3 OBJECTIVES OF THE RESEARCH

a) To investigate the effect of processing parameters on solidification rate and fraction solid and in turn the microstructure of produced SSM wrought aluminium feedstock billets.
b) To determine the liquidus, eutectic and solidus temperature, fraction solids and dendritic coherency point resulting from the different cooling conditions of wrought aluminium alloy.
c) To evaluate the microstructure formation and mechanical properties of the wrought aluminium formed components.

1.4 HYPOTHESIS

An important metallurgical characteristic that has significant effect during SSM processing is a fraction solid. The fraction solid determines material flowability and influence microstructure and defect formation. The low viscosity (low fraction solid volume) component helps material to flow inside die cavity. Meanwhile, high fraction solid volume helps to prevent various defects, a finer internal structure and a high quality product. This fraction solid however is found highly depended on material processing parameters. Hence, in order to produce better quality component with the combination of excellent flowability and superior mechanical properties, the fraction solid volume during SSM processing need to be controlled. This can be achieved by executing adequate processing parameters during SSM processing.

CHAPTER 2

RELATED TECHNICAL PAPER 1

Thermal Analysis of Aluminium 7075 prior to Semisolid Metal Processing

N A Razak[1,a)], A H Ahmad[1,b)], and M M Rashidi[1,c)]

[1]*Manufacturing Focus Group, Faculty of Mechanical Engineering, Universiti Malaysia Pahang, 26600 Pekan, Pahang, Malaysia.*

[a)]*Corresponding author: azhani@ump.edu.my*
[b)]asnul@ump.edu.my
[c)]mrashidi@ump.edu.my

Abstract. Thermal analysis method is broadly used to determine solidification characteristics of metals and alloys in numerous metallurgical processes. This paper presents the relationship between fraction solid and temperature of wrought aluminium 7075 alloy at different cooling rate conditions. The 7075 was heated in a graphite crucible to a temperature of 750 °C by an induction heating machine. A K-type thermocouple was located at the center of the crucible and was immersed within the molten metal to a depth of 15 mm from the top of the graphite crucible. The temperature and time profiles were recorded with a Data Logger GL-220 which was connected to a notebook with GL software. Three different cooling rate conditions (normal, intermediate, and high) were carried out with the crucible was set in the open atmosphere, in open atmosphere with minimum airflow over the crucible, and in open atmosphere with maximum airflow over the crucible, respectively. Based on the obtained cooling curves data, the enthalpy of phase change at respective temperature was determined. Results show that the calculated cooling rates for normal, intermediate, and high cooling rates were at 2.23 °C/s, 2.88 °C/s, and 3.20 °C/s respectively. The variations of cooling rate were found directly related to phase transformation during solidification including at liquidus, eutectic and solidus temperatures.

Introduction

The SSM processing is an attracting technology, which enables the production of near net shape components with superior quality as compared to conventional casting process [1]. Most of the materials used in the SSM processing techniques are cast aluminium alloys such as A356 and A357 due to their good fluidity [2–6]. Nevertheless, they have relatively poor mechanical properties as compared to wrought aluminium alloys. Therefore, there is a strong drive to use 7XXX series aluminium alloys in SSM processing [7–10] as they have the highest mechanical properties among aluminium alloys [11].

Quality of the feedstock billets during SSM processing needs to be controlled, just like in conventional casting. Thermal analysis (TA) is one of the useful and vital characterization techniques used to record physical properties of the sample as a function of temperature versus time or thermal curve either sample is heated or cooled by using a scheduled program [12]. This measurement aims to assess the changes that occurred in the sample for both physical and chemical aspects based on the measured properties of thermal analysis curve. The quality of a melt batch is observed via a recorded phase change temperatures and, fraction solid and temperature profiles relations [13]. Several techniques are also available to investigate the solidification of metals and alloys, and among them are differential scanning calorimetry (DSC) and differential thermal analysis (DTA). Aside from those methods, Bäckerud et. al. has introduced a different approach with two thermocouples to measure heat change in a single sample [14]. This method has enabled in-situ measurement and provides the actual heat

change in a test sample. Another way for investigating solidification of metals and alloys is the cooling curve analysis method. This technique determines the relationship between melt treatment, alloy composition, cooling curve parameters and properties. This technique has been widely used to determine material thermal profiles in these recent years [15–18]. The determination of a baseline is vital in cooling curve analysis method as it will decide the fraction solid and temperature relations. The cooling curve analysis technique interprets latent heat that evolved during solidification by the first derivation of cooling curve graph. This latent heat, which was characterized by the temperature change inside the molten metal, represented the phase changes [13].

Chen et. al., had done a study on the effect of cooling rate on solidification parameters and microstructure of Al-Si alloy with the cooling curve technique [19]. They revealed that cooling rate was the main factor that affects the temperature gradient and solidification rate, which in turn affect the microstructure and mechanical properties of castings. However, there is still a lack of detail experimental investigations on the thermal profiles of aluminium 7075 at various sample mass and solidification rates. Hence, this experimental works aims to understand the relationship between solidification rate, and fraction solid development at different cooling rate conditions. The resulted output from this study is essential in selecting or determining the best processing parameters for thixoforming process.

EXPERIMENTAL PROCEDURE

TABLE 1. Chemical compositions of wrought aluminium 7075 alloy from the experiment and literature.

Source (wt%)	Al	Cr	Cu	Fe	Mg	Mn	Si	Ti	Zn
As-received sample	89.8	0.27	1.33	0.22	2.26	0.05	0.16	0.07	5.74
Ahmad [20]	88.5	0.2	2.02	0.24	2.38	0.12	0.14	0.09	6.04
Bäckerud [14]	Bal	0.19	1.36	0.28	2.49	-	0.11	-	-
ASM [21]	87.1-91.4	0.18-0.28	1.2-2.0	<0.5	2.1-2.9	<0.3	<0.4	<0.2	5.1-6.1

Wrought aluminium 7075 alloy was used in this experimental work and its chemical composition was determined with Optical Emission Spectroscopy, Foundry Master Oxford Instruments. The chemical composition test of the alloy was repeated six times for the purpose of accuracy and was then compared with the literature. Table 1 shows the chemical compositions of the 7075 used in this experiment and from the literature.

The 7075 with 20 g in weight was placed in a 20 mm inner diameter and mm in height graphite crucible. The graphite crucible then was heated to a temperature of 750 °C with a KX-5188 series auto control high frequency induction heating machine. After the 7075 melted inside the graphite crucible, three different cooling conditions were selected. First, the crucible was allowed to cool naturally at room temperature to achieve a normal cooling rate. The other two conditions, which were the intermediate and high cooling rate, were conducted with the graphite crucible with molten alloy in a forced air flow with slower and faster speeds, respectively. A K-type thermocouple was positioned at the center of the crucible. It was immersed within the metal to a depth of 15 mm from the top of the melt. A Data Logger GL-220 which was connected to a notebook was used to record the temperature versus time cooling curve data. The data logger was set at 10 Hz/ch. Cooling rates were determined from the cooling curve, which were chosen above the liquidus temperature. The selected regions for calculation of cooling rates were set between 10 to 50 °C above the liquidus temperature. Calibration of the thermocouple was done before each cooling conditions were recorded to ensure accurate readings. The thermal analysis experiments for each condition were repeated three times to ensure reproducibility of the results and the setup for thermal analysis is shown in Fig. 1.

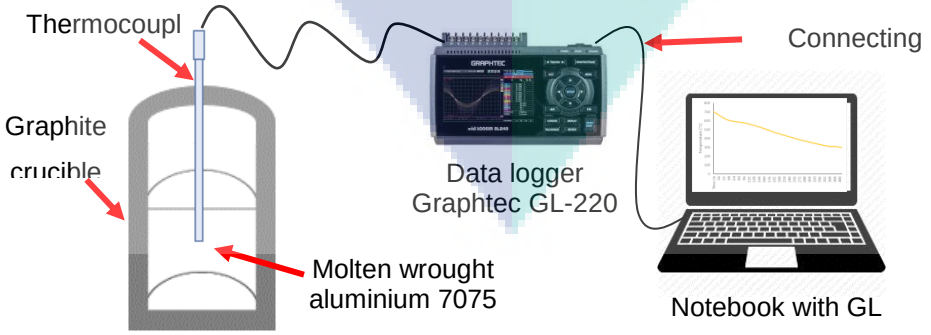

FIGURE 1. Schematic illustration of thermal analysis experiment setup for normal cooling condition.

OriginPro 9 data analysis software was used to plot the cooling curve and first derivative curve (dT/dt curve). A base line was constructed on the first derivative curve to represent the cooling rate which would have occurred if the latent heat evolution was not present. The base line follows the same trend line with the first

derivative curve in the single-phase regions, which are regions above the liquidus temperature, and below solidus temperature [13]. Fraction solid (f_s) at specific times (Δt) was then computed by dividing the area integration value at Δt with the total area integration values measured from the start (liquidus temperature) to end (solidus temperature) of solidification as shown in Eq. (1), where *cc* and *bc* is a cooling curve and baseline curve, respectively.

$$f_s = \frac{\int_{t_0}^{t_1} dH}{\int_{t_0}^{t_f} dH} = \frac{\int_{t_0}^{t_1} \left[\left. \frac{dT}{dt} \right|_{cc} - \left. \frac{dT}{dt} \right|_{bc} \right] dt}{\int_{t_0}^{t_f} \left[\left. \frac{dT}{dt} \right|_{cc} - \left. \frac{dT}{dt} \right|_{bc} \right] dt} \tag{1}$$

RESULTS AND DISCUSSION

Figure 2 (a) and (b) represents the cooling curve, its corresponding first derivative curve alongside with baseline curve, and fraction solid recorded during solidification of a normal cooling rate condition. Cooling rate was found to be at 2.23 °C/s, which was measured by the slope of the cooling curve above the liquidus region. Based on Fig. 2 (a), the liquidus, eutectic, and solidus temperature of the normal cooling rate condition were recorded at 619.30, 438.48, and 421.90 °C, respectively. Meanwhile, the purpose of first derivative curve is to assist in identifying the changes of phases during solidification process, which might not be noticed just by using only the cooling curve. Fraction solid values which were calculated between liquidus and solidus region is shown in Fig. 2 (b). The information on fraction solid that happens during progressive solidification is useful to determine the processing temperature settings for semisolid metal processing.

Figure 3 (a) shows the cooling curve for an intermediate cooling rate condition. The cooling rate was calculated at several points before liquidus temperature and was found to be at 2.88 °C/s. Based on the figure, the liquidus, eutectic and solidus temperature occurred at 603.84 °C, 415 °C, and 393.93 °C respectively. The corresponding calculated relations of temperature – fraction solid (Ta − fs) is presented in Fig. 3 (b).

The cooling curve for high cooling rate condition which was found to be 3.20 °C/s is shown in Fig. 4 (a). The liquidus, eutectic and solidus temperature were recorded at 589.91 °C, 405.55 °C and 385.60 °C respectively. The first derivation of the cooling curve with a baseline were also shown in Fig. 4 (a). Whereas, the corresponding calculated relations of temperature – fraction solid (Ta − fs) is presented in Figure 4 (b).

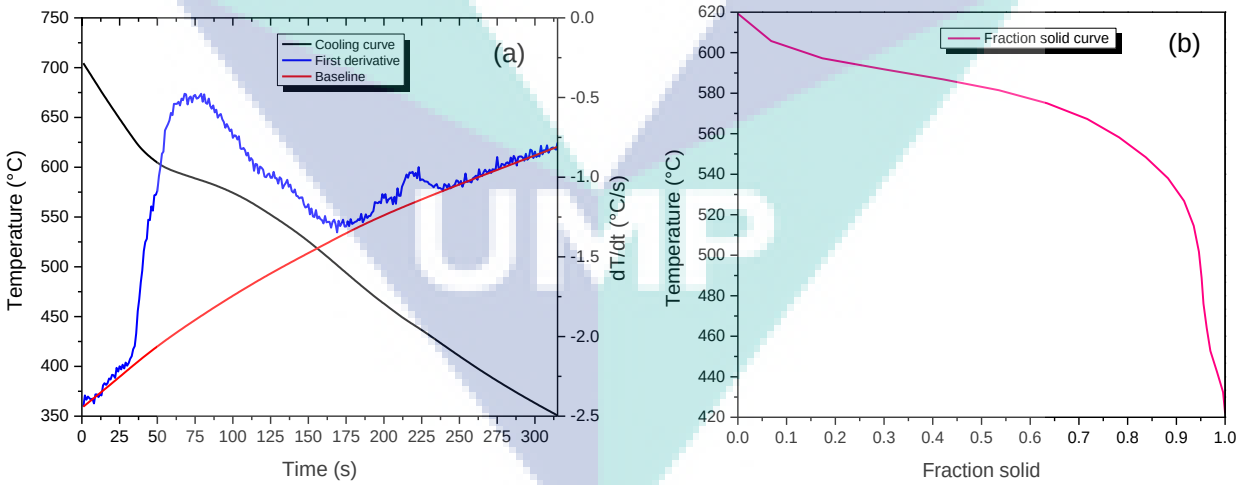

FIGURE 2. Thermal analysis results for a cooling rate of 2.23 °C/s, with the (a) cooling curve, cooling curve derivation, and baseline with respect to time, and (b) calculated temperature-fraction solid relation.

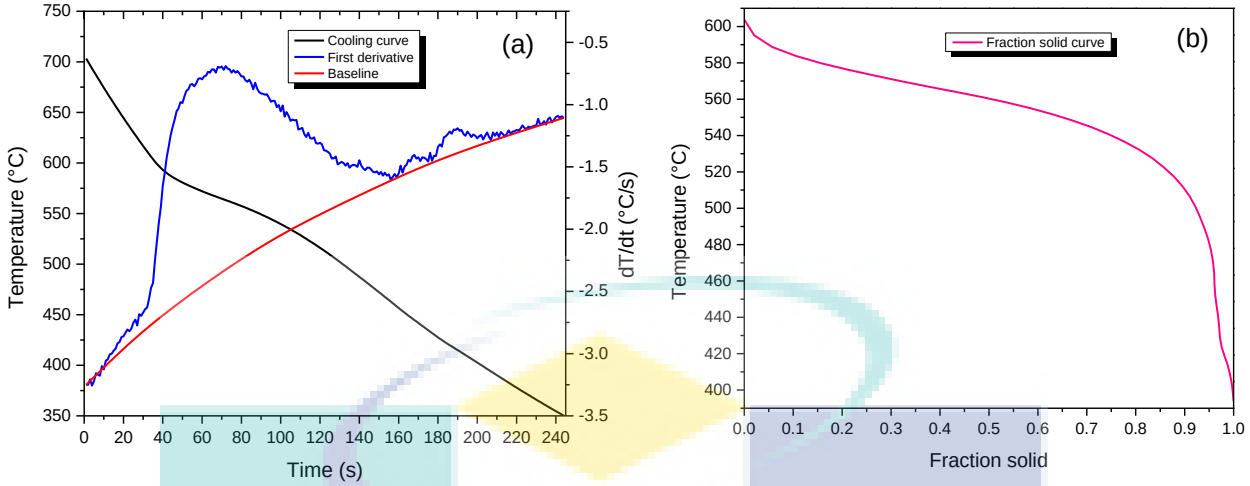

FIGURE 3. Thermal analysis results for a cooling rate of 2.88 °C/s, with the (a) cooling curve, cooling curve derivation, and baseline with respect to time, and (b) calculated temperature-fraction solid relation.

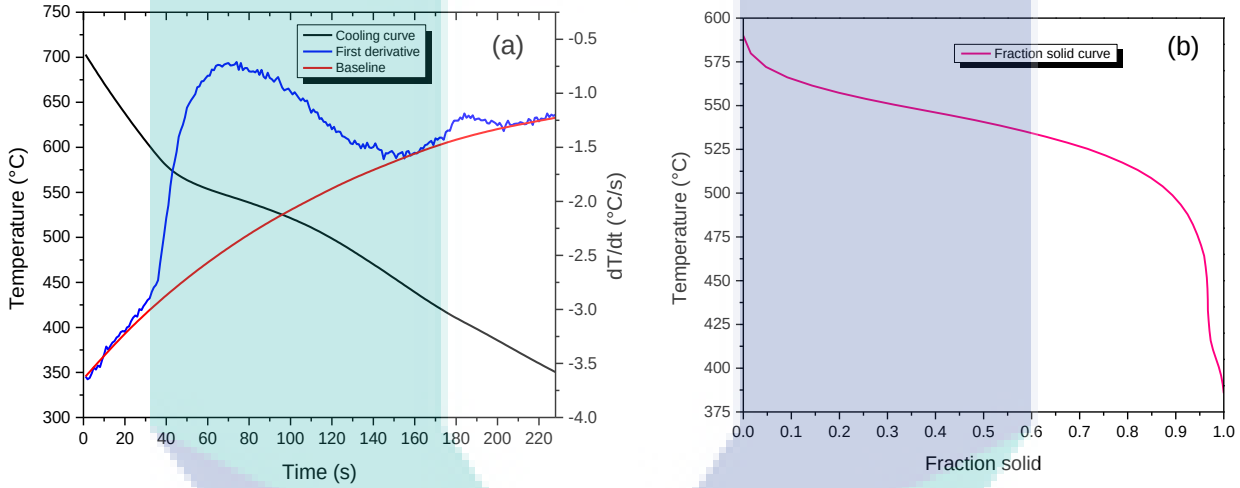

FIGURE 4. Thermal analysis results for a cooling rate of 3.20 °C/s, with the (a) cooling curve, cooling curve derivation, and baseline with respect to time, and (b) calculated temperature-fraction solid relation.

TABLE 2. Liquidus, eutectic, and solidus temperature at different cooling rate conditions.

Source	Cooling rate (°C/s)	Liquidus temperature (°C)	Eutectic temperature (°C)	Solidus temperature (°C)
This work	2.23	619.30	438.48	421.90
This work	2.88	603.84	415.0	393.93
This work	3.20	589.91	405.55	385.69
Bäckerud [14]	2.3	628.0	466.0	466.0
ASM [21]	-	635.0	-	477.0

The liquidus, eutectic, and solidus temperatures of various cooling rate conditions for this experimental work, alongside with data from other reports are shown in Table 2. The results in Table 2 show that the liquidus, eutectic and solidus temperature for this work are slightly lower than other results from the literature. Even though the cooling rate used between this work and from the literature are quite similar, but the mass of molten alloys contributes to the results dissimilarity. It was found that the mass of molten alloys that have been used by Bäckerud was 60 g rather than 20 g used in this work [14]. This mass factor explained well about the variation between these two results.

CONCLUSIONS

The thermal analysis with different cooling rates was successfully investigated. The difference in cooling rate conditions has a significant effect to the changes of phases during solidification process. The liquidus, eutectic, and solidus temperature for a normal cooling rate (2.23 °C/s) occurred at 619.30 °C, 438.48 °C, and 421.90 °C whilst for intermediate cooling rate (2.88 °C/s) occurred at 603.84 °C, 415.0 °C, and 393.93 °C, respectively. The liquidus, eutectic, and solidus temperature for a high cooling rate (3.20 °C/s) were recorded at a lower temperature than the other cooling rate conditions which were at 589.91 °C, 405.55 °C, and 385.69 °C.

ACKNOWLEDGMENTS

The authors would also like to acknowledge the support from Universiti Malaysia Pahang (RDU1603125) and Ministry of Higher Education Malaysia (RAGS2015-1) for funding this work.

REFERENCES

[1] D.H. Kirkwood, P. Kapranos, Semisolid Processing, in: S. Hashmi (Ed.), Ref. Modul. Mater. Sci. Mater. Eng., Elsevier Inc., Oxford, UK, 2016: pp. 1–8.
[2] Y. Birol, J. Alloys Compd. 486 (2009) 173–177.
[3] Y. Birol, J. Alloys Compd. 473 (2009) 133–138.
[4] O. Lashkari, The Rheological Behavior of Semi-Solid A356 Alloy, (Canada: Universite du Quebec a Chicoutimi, 2006).
[5] J. Wannasin, S. Thanabumrungkul, Songklanakarin J. Sci. Technol. 30 (2008) 215–220.
[6] A. Kolahdooz, S. Nourouzi, M. Bakhshi Jooybari, S.J. Hosseinipour, Experimental investigation of the effect of temperature in semisolid casting using cooling slope method, Proc. Inst. Mech. Eng. Part E J. Process Mech. Eng. 230 (2016) 1–10.
[7] Rogal, J. Dutkiewicz, H. V. Atkinson, L. Lityńska-Dobrzyńska, T. Czeppe, M. Modigell, Mater. Sci. Eng. A. 580 (2013) 362–373.
[8] S. Chayong, H. V. Atkinson, P. Kapranos, Mater. Sci. Eng. A. 390 (2005) 3–12.
[9] S. Chayong, H. Atkinson, P. Kapranos, S. Chayong, H. Atkinson, Mater. Sci. Technol. 20 (2004) 490–496.
[10] L. Yageng, M. Weimin, Z. Wenzhi, Y. Bin, China Foundry. 11 (2014) 79–84.
[11] I.J. Polmear, Light Alloys, From Traditional Alloys to Nanocrystals, Fourth, (Oxford: Butterworth-Heinemann, 2006).
[12] M.E. Brown, Introduction to Thermal Analysis:Techniques and Applications, (Kluwer Academic Publishers, Dordrecht, 2004).
[13] D. Emadi, L. V. Whiting, S. Nafisi, R. Ghomashchi, J. Therm. Anal. Calorim. 81 (2005) 235–242.
[14] L. Bäckerud, E. Król, J. Tamminen, Solidification Characteristics of Aluminium Alloys; Volume 1: Wrought Alloys, (Oslo: Skan Aluminium, 1986).
[15] S. Farahany, H.R. Bakhsheshi-Rad, M.H. Idris, M.R. Abdul Kadir, A.F. Lotfabadi, A. Ourdjini, Thermochim. Acta. 527 (2012) 180–189.
[16] V.A. Hosseini, S.G. Shabestari, R. Gholizadeh, Mater. Des. 50 (2013) 7–14.
[17] Ihsan-ul-haq, J.-S. Shin, Z.-H. Lee, Met. Mater. Int. 10 (2004) 89–96.
[18] S.G. Shabestari, M. Malekan, Can. Metall. Q. 44 (2005) 305–312.
[19] R. Chen, Y. Shi, Q. Xu, B. Liu, Trans. Nonferrous Met. Soc. China. 24 (2014) 1645–1652.
[20] A.H. Ahmad, S. Naher, D. Brabazon, Key Eng. Mater. 554–557 (2013) 582–595.
[21] ASM International, ASM Metals Handbook, Properties and Selection:Nonferrous Alloys and Special-Purpose Materials, Tenth (Materials Park, OH: ASM International, 1990).

CHAPTER 3

RELATED TECHNICAL PAPER 2

Preparation of aluminium 7075 feedstock billets via direct thermal method for semisolid metal processing

A. H. Ahmad[a*], N. A. Razak[a] , M.M. Rashidi[a], S. Naher[c], D. Brabazon[b]

[a]*Faculty of Mechanical Engineering, Universiti Malaysia Pahang, Pekan, 26600, Pahang, Malaysia*
[b]*School of Mechanical and Manufacturing Engineering, Dublin City University, Glasnevin, Dublin 9, Ireland*
[c] *School of Mathematics, Computer Science & Engineering,, City University of London, Northampton Square, EC1V 0HB, London, United Kingdom*

ABSTRACT

The evolution of microstructure affects from different pouring temperatures and holding times using a direct thermal method is presented in this paper. The direct thermal method is one of the thermal technique which is used to produce semi-solid metal feedstock. In this experimental work, aluminium 7075 alloy was used. The experiments were carried out by pouring 7075 molten alloys into a cylindrical copper mould at different pouring temperatures of 685 °C, 665 °C and 645 °C meanwhile the holding time of 20 s, 40 s and 60 s before quenched into room temperature water. The sample with pouring temperature 680 °C and holding time 20 s produced the smallest primary phase structure size. Nevertheless, the combination between pouring temperature and holding time of 665 and 60 s respectively produced the highest circularity value.

Keywords: Semisolid metal, aluminium 7075, direct thermal method, globular microstructure

1. INTRODUCTION

Semi-solid metal (SSM) processing occurs between the liquidus and solidus temperature, a range within which the fluidity of molten metal can change greatly. Instead of a dendrite microstructure from the conventional liquid casting, a globular or spheroidal microstructure can be achieved by controlling process parameters, such as the temperature of the melt, cooling rate, stirring time, stirring

type, and stirring speed [1,2]. The flow behavior of SSM was influenced by the primary phase morphology of SSM slurries [3,4]. Study on SSM flowability shows dendritic structures tend to have the lower flowability than equiaxed structures [5]. The dendritic structures have a tendency to interlock each other and prohibited material from flows when an external force is applied. Furthermore, non-dendritic or globular structures were able to flow better which they tend to rotate and slip during forming operation [6,7]. A finer microstructure produced a better flowability due to better movement, less collisions among particles and lower viscosity [1,4,7]. Several rheological tests were performed in order to characterize SSM behavior. Simple model and defined parameters to characterize rheological of the SSM slurries were used in several parameters to characterize rheological of the SSM slurries were used in several research with variance in particle sizes to calculate the effective fraction solid.

SSM casting processes have developed as a niche-casting process where high mechanical properties or a complex shape, or both, are required. It is an advanced technology which offers the ability to produce various components to be used in different industries, mostly within the automotive and aerospace industries. This process has many advantages, including low processing temperature, making it energy efficient, which contributes to part cost saving [2,8–10]. Due to increased fluidity during forming, provide from the spheroidal microstructure, parts formed have lower porosity levels [11] and associated improved mechanical properties [12]. Other benefits include a die-life extension [13], less filling defects, and faster solidification [14]. From a productivity viewpoint, SSM processing can provide the same or a greater production rate compared to conventional high-pressure die casting processes.

The novel process of Direct Thermal Method (DTM) was discovered initially by Brabazon and co-workers in 1997 [15]. In this process, the aluminium alloy was cooled from a low superheat within thin-walled cylindrical copper moulds. The superheated aluminium was rapidly cooled into the semi-solid state by the heat extraction provided by the copper mould. This initial rapid cooling gave rise to copious nucleation. At the same time, a thermal equilibrium was rapidly reached between the copper mould and the aluminium alloy which in effect provided an isothermal arrest which enabled the diffusion dominated processes of ripening to yield a globular microstructure. The concept of this process is different from the others in that it uses only natural cooling.

Important processing parameters in DTM that shape the desirable microstructure include pouring temperature, holding time before quenching or forming, and size of cooling mould utilized. Lower pouring temperature and shorter holding periods produced more spherical structures [16]. The more spheroidal primary phase would increase the fluidity of the material during SSM forming. Higher cooling rates resulting from lower pouring temperatures above to below the liquidus temperature provide less superheat to be extracted by cylindrical copper mould. The resulting increased undercooling of the alloy during the solidification stage promotes the formation of more nuclei which in turn results in a smaller grain size [16]. An obvious advantage of this process is that it needs no special equipment and provides for low processing cost. However, there are limitations on the size of billet that can be produced.

Recently, wrought aluminium alloys receive greater attention by the researchers for SSM processing [10,14,17–21]. Among commercial wrought aluminium alloys, 7xxx series alloys (Al-Zn-Mg-Cu) are regarded as excellent candidate

materials for structural automotive applications due to their high strength-to-weight ratio, good ductility, and excellent corrosion resistance in most environments [10]. Aluminium 7075 has recently been investigated for use in the SSM processing [14,22–27]. The performance of aluminium 7075 has been studied by using both thixoformed cooling slope and recrystallization and partial melting (RAP) route in order to compare their mechanical properties [24]. It was noted in this work that thixoformed RAP route produced better tensile properties.

The aim of this work is to investigate the effect of processing parameter to the microstructure of wrought aluminium 7075 which processed by using DTM. In particular, the microstructure evolution was also investigated.

1. Experimental procedure

The chemical composition of the aluminium 7075 alloys used in this experimental work, as determined by Optical Emission Spectroscopy, Foundry Master Oxford Instruments and from the literature, is presented in Table 1. The 7075 was supplied by Impact Ireland (Metals) Ltd, Ireland. The chemical composition test was repeated five times in order to acquire accurate results.

The following procedures conducted the experiment setup for DTM. A 1 kg aluminium 7075 ingots were placed in a graphite crucible and were heated to a temperature of 700 °C by using the resistance heated Carbolite 1600 box furnace. Once the desired temperature of the melt was obtained, it was poured into a cylindrical copper mould with 1 mm wall thickness, 25 mm in diameter, and 100 mm in height. The different pouring temperatures were set at 645 °C, 665 °C or 685 °C. After pouring molten metal into the mould, it was held for 20 s, 40 s or 60 s respectively. After the holding time for each copper mould was achieved, it later quenched into room temperature water. In order to capture microstructure for the billet with the normal solidification condition, another billet which poured with 685 °C molten alloy was allowed to solidify without quenching.

Table 1 Chemical composition of aluminium 7075 from the experiment and literature.

Source (wt%)	Al	Cr	Cu	Fe	Mg	Mn	Si	Ti	Zn
Experiment	88.5	0.2	2.02	0.24	2.38	0.12	0.14	0.09	6.04
Bäckerud [28]	Bal	0.19	1.36	0.28	2.49	-	0.11	-	-
ASM [29]	87.1-91.4	0.18-0.28	1.2-2.0	<0.5	2.1-2.9	<0.3	<0.4	<0.2	5.1-6.1

Solidified alloy of the DTM sample with initial dimensions of 25 mm in diameter and 100 mm in length were removed from the copper moulds and later machined by a Computer Numerical Control (CNC) lathe machine at 20 mm from the top and 5 mm from the bottom of the DTM sample. These locations were selected in order to give a minimum balance of 75 mm for the final DTM feedstock billets. The micrograph samples for each solidified alloy were obtained from the end of surface which sliced at 20 mm from the top. The schematic for DTM feedstock billet machining dimensions are shown in Fig. 1.

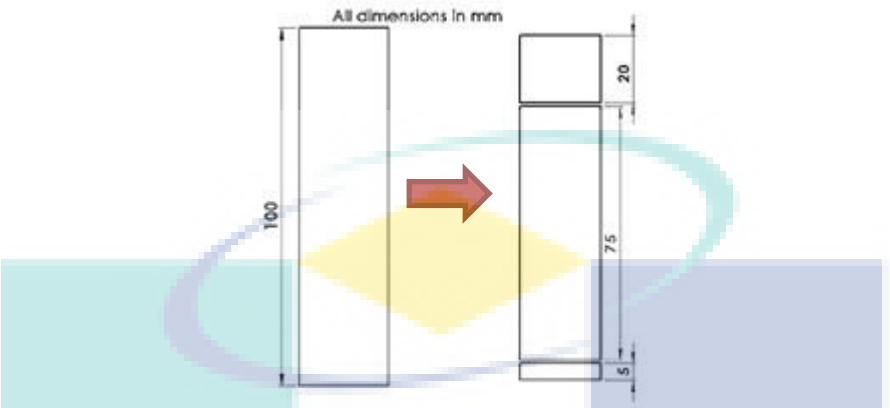

Fig. 1. Schematic for feedstock billet after DTM with initial and final dimensions.

Samples were mounted to provide protection to sample and to create a uniform surface for subsequent automatic grinding and polishing processes. The samples mounted with Bakelite thermoset phenolic resin by using Buehler Simplimet 2000 Mounting Press hot mounting machine. The curing temperature was set at 180 °C for 8 minutes and cooled for 4 minutes.

Mounted samples were ground by using 240, 800, and 1200-grit size silicon carbide (SiC) for 4 minutes, at 10 N force pressure at a 200-rpm grinding wheel speed with flowing water. The flowing water helps to remove heat and flush any loose particles of metals and abrasive. These initial polishing steps are called planar grinding.

Ground samples were then polished by the Ultra Pad with 9 and 3 micron; and Acetate Silk with 1 micron size diamond suspension. The samples were then given a final polish with Chemomet with 0.05 micron size alumina polishing suspension for 6 minutes each, at 10 N pressures and the polishing speed of 150 rpm. Buehler Motopol 2000 grinder/polishing machine were used to perform both of grinding and polishing works.

Chemical etching was used to reveal the grain boundaries of the material under an optical microscope after the polishing process. During the grinding and polishing processes, thin layer on the material surface was formed. The chemical etching removed this thin layer by attacking the surface with the highest energy leading to surface relief that to be distinguished under the reflective light. The samples then were etched by using Keller's etch for approximately 30 seconds [29]. Compositions of the etchant were 95 ml water, 1 ml hydrofluoric acid HF, 1.5 ml hydrochloric acid HCL and 2.5 ml nitric acid HNO_3.

Reichert ME F2 universal camera optical microscope was used to view the microstructures. Buhler Omnimet Enterprise software was then used to capture the microstructure images by using a 8x, 10x, 20x and 40x magnification.

Primary phase grain size diameter, circularity, aspect ratio and secondary phase area measurement were determined by Image J software. The circularity is an indication of a perfect circle which occurs within a microstructure. The value that approaches a value of 1.0 is considered as the perfect circle with decreasing number toward 0.0 is indicates an increasing elongated shape. The aspect ratio is

an indication for circular or square morphology, which aspect ratio value increases with an elongated particle. The circularity, C and aspect ratio, AR were calculated by using the following formula as in Eq. (1) and Eq. (2) which P and A are representing a perimeter and an area of the particle respectively:

$$\mathrm{C} = 4\pi A/P^2 \tag{1}$$

$$\mathrm{AR} = \text{major axis}/\text{minor axis} \tag{2}$$

The Energy-dispersive X-ray Spectroscopy (EDXS) analysis was performed by an Oxford Instrument Inca Energy 350XT machine. This system uses a Carl-Zeiss EVO-LS15 Scanning Electron Microscope (SEM) to observe the sample structure while EDXS detectors disperse chemical composition data. The EDXS detector and sample surface were set less than 11 mm in order to collect sufficient data. The data which obtained from the EDXS detector were then analysed by Inca Software.

2. Results

Microstructure for a starting material is shown in Fig.. The grain structure formation was elongated and un-recrystallized. These grain structure formations were shown by the contrast of variations with the formation of elongated grains, with several porosities detected.

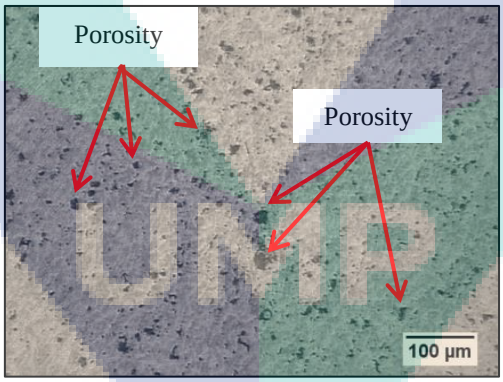

Fig. 2. As received sample for aluminium 7075.

Comparison between DTM samples was made by examining the microstructure formation which occurred within DTM samples. The microstructure for pouring temperature of 685 °C, 665 °C and 645 °C with holding time of 60 s, 40 s and 20 s are presented in Fig. 3 to Fig. 5 respectively. Likewise, the microstructure for pouring temperature of 685 °C which was allowed to solidify without quenching is shown in Fig. 6.

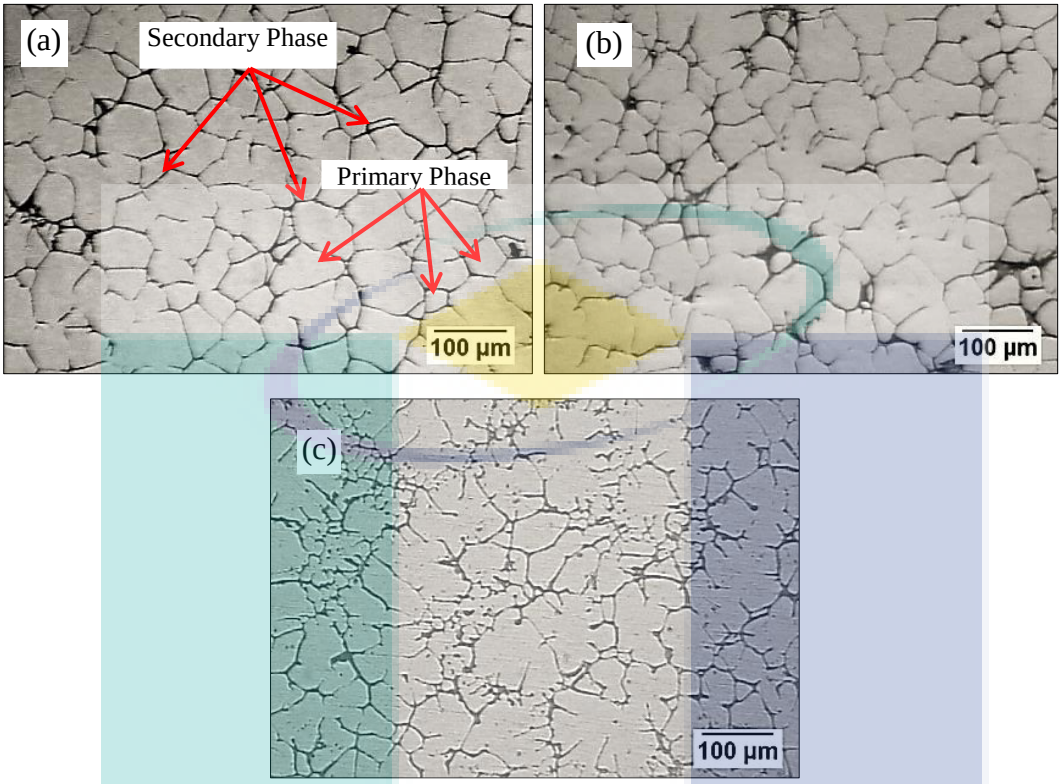

Fig. 3. Microstructure for sample with pouring temperature of 685 °C and at different holding time with (a) 60 s (sample 1), (b) 40 s (sample 2) and (c) 20 s (sample 3).

The role of holding time in DTM was to ensure an adequate temperature was achieved before quenching. The quenching temperature for each mould was estimated accordingly as the temperature in the copper mould was dropped at 0.7 °C/s, which was obtained from a separate experimental work [30]. The first calculated quenching temperatures for pouring temperature of 685 °C by the holding time of 60 s, 40 s and 20 s were at 643 °C, 657 °C and 671 °C respectively. The second calculated quenching temperatures for pouring temperature of 665 °C by the holding time of 60 s, 40 s and 20 s were at 623 °C, 637 °C and 651 °C. The last calculated quenching temperatures for pouring temperature of 645 °C by the holding time of 60 s, 40 s and 20 s were at 603 °C, 617 °C and 631 °C respectively. These quenching temperatures later were used to determine $T_a - f_s$ relations within copper mould which were based on the results obtained from a previous experiment [31].

There was an apparent indication from these figures that there was a significant microstructure difference between samples that quenched at different time period. Another obvious finding with these results was the sample which allowed to solidify without quenching produced a bigger size structure than other samples. The microstructure between the sample with pouring temperature of 685 °C, holding time of 60 s and sample without quenching show this evidence as presented in Fig. 3 (a) and Fig. 6.

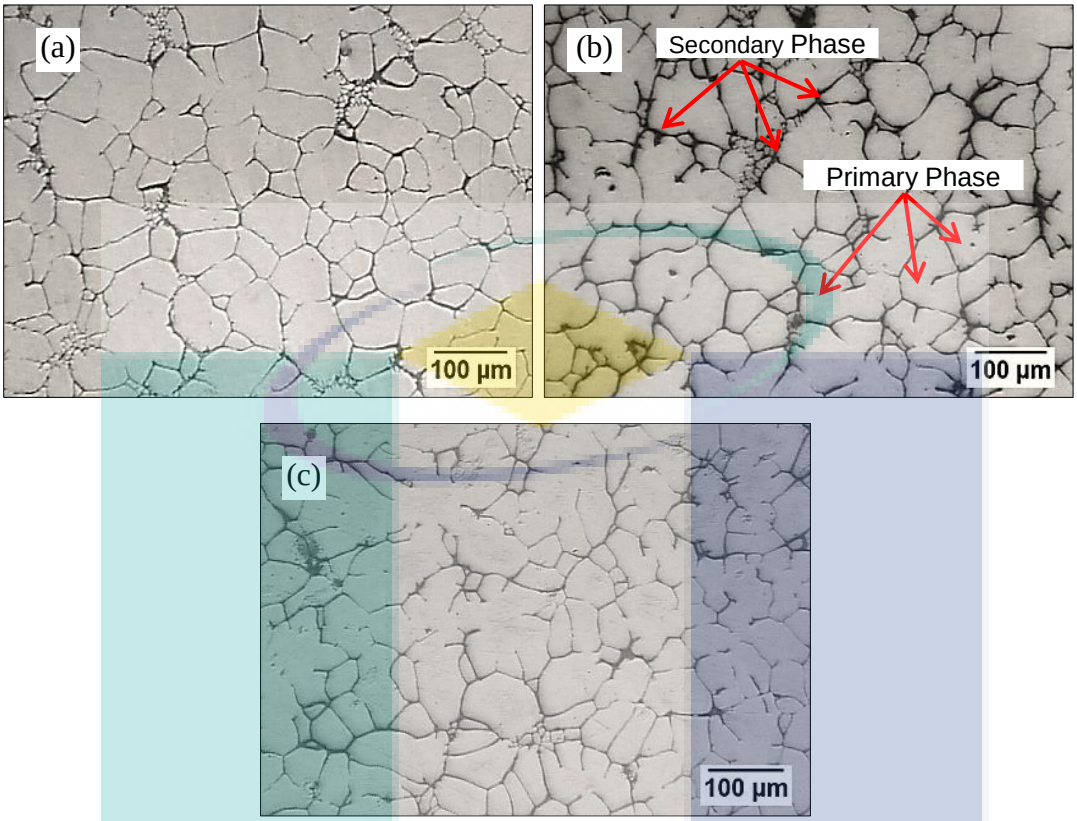

Fig. 4. Microstructure for sample with pouring temperature of 665 °C and at different holding time with (a) 60 s (sample 4), (b) 40 s (sample 5), and (c) 20 s (sample 6).

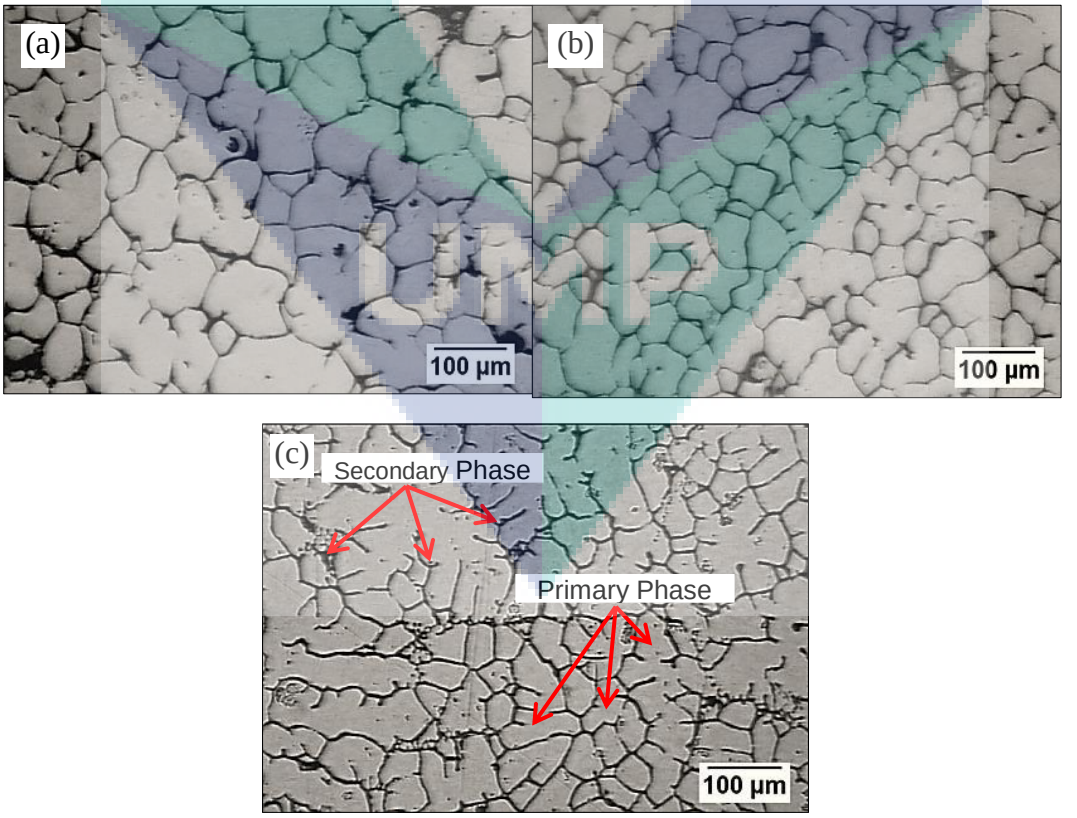

Fig. 5. Microstructure for sample with pouring temperature of 645 °C and at different holding time with (a) 60 s (sample 7), (b) 40 s (sample 8), and (c) 20 s (sample 9).

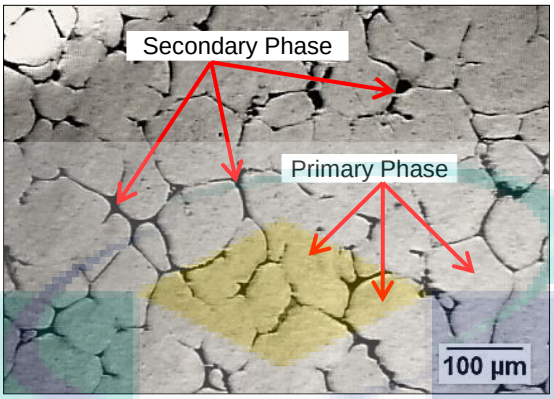

Fig. 6. Microstructure for sample with pouring temperature of 685 °C (sample 10) and allowed to solidify to room temperature.

Comparisons between the microstructure of the samples were made by using a grain size measurement method. The grain size measurements consist of the average values for primary grain diameter, circularity, aspect ratio and secondary phase area. The results obtained from the grain size measurement are presented in Fig. 7 to Fig. 10.

There was a significant difference between average microstructure primary grain diameters for sample 1, 2 and 3 which are presented in Fig. 7. Moreover, the significant difference was also found with sample 10 that allowed to solidify without quenching when the comparison was made with other samples. Sample 10 which processed with pouring temperature of 685 °C obtained the highest average diameter value. This gives the indication that sample 10 contained large microstructure features. There was the insignificant difference for grain diameter with sample 3 to 9 which processed at different processing conditions. The results were found overlapped to each other. Together, these results provide an important indicator that the relationship between processing parameters and microstructure formation.

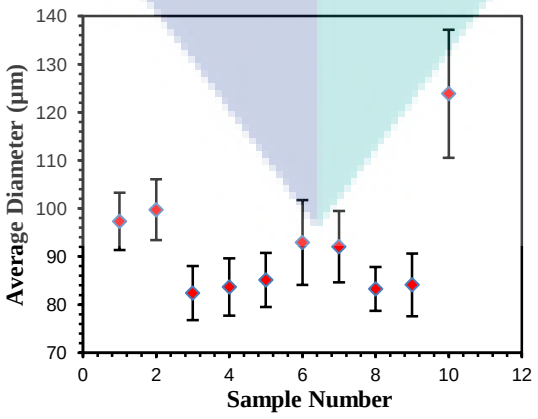

Fig. 7. Grain size measurement for the average primary grain diameter of 10 samples (errors are 95% confidence intervals).

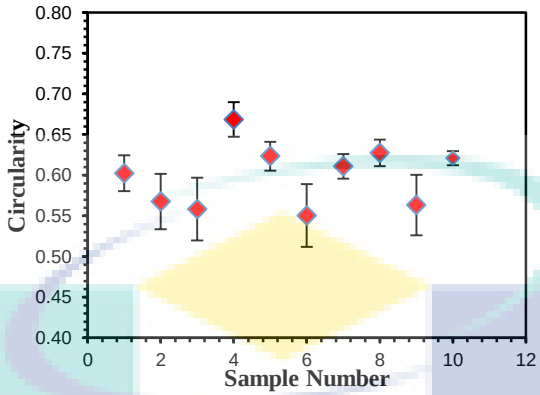

Fig. 8. Grain size measurement for the average microstructure circularityof 10 samples (errors are 95% confidence intervals).

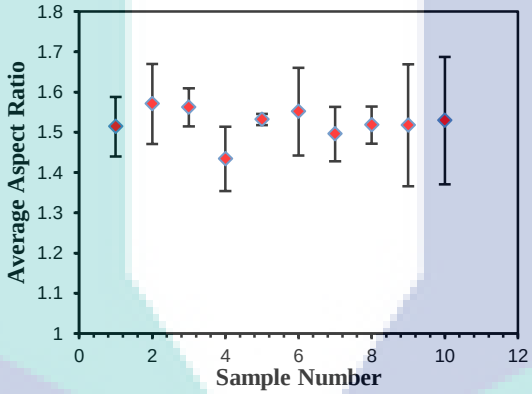

Fig. 9. Grain size measurement for the average microstructure aspect ratio of 10 samples (errors are 95% confidence intervals).

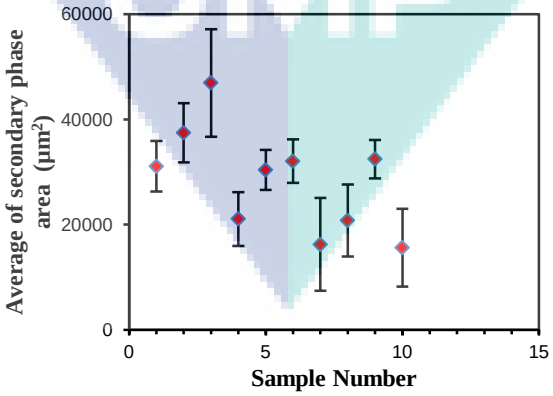

Fig. 10. Grain size measurement for the secondary phase area of 10 samples (errors are 95% confidence intervals).

In order to assess the chemical compositions of the sample, an Energy-dispersive X-ray Spectroscopy (EDXS) analysis was used. The test was performed on two different areas consist of primary and secondary phases. The primary phase was represented by a solid grain structure as shown in Fig. 11. Meanwhile, the secondary phase was represented by liquid structures that occurred at the grain boundary of the solid grain structure as shown in Fig. 12. The chemical compositions of one of DTM samples at primary phase, which analysed by using EDXS are shown in Table 2. Three major elements were detected consist of aluminium (Al), Zinc (Zn) and Magnesium (Mg).

Nevertheless, chemical compositions of one of DTM samples at secondary phase, which analysed by using EDXS are shown in Table 3. Two major elements were detected consist of aluminium (Al) and copper (Cu).

Table 2 Chemical composition of primary phase from EXDS.

Elements (wt%)	**Al**	**Zn**	**Mg**
Spectrum	92.71 - 100	3.40 – 5.95	1.59 – 1.89

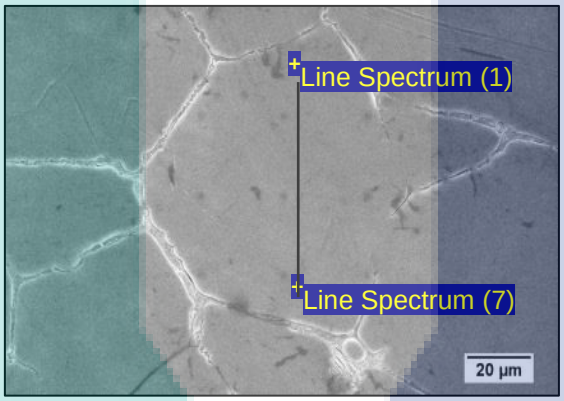

Fig. 11. EDXS line spectrum for Primary phase.

Table 3 Chemical composition of secondary phase from EDXS.

Elements (wt%)	**Al**	**Cu**
Spectrum	45.47 – 63.18	36.82 – 54.25

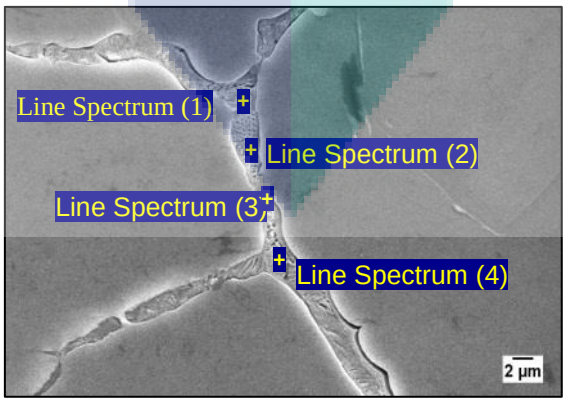

Fig. 12. EDXS line spectrum for secondary phase.

3. Discussion

4.1 Effect of Pouring Temperature

The variation of pouring temperature used in DTM experiment was intentionally established to determine the effect of processing parameters to microstructure formation. The results of this experimental work indicated that the grain sizes of the sample were strongly influenced by the processing parameters applied. Prior study has noted that the pouring temperature was among the important factors in DTM which determined the success of the process [31].

The pouring temperature is related to the cooling rate. Lower pouring temperature is the important parameter in producing a globular microstructure in the DTM. Lower pouring temperature for DTM retards the formation of microstructure [31]. Lower pouring temperature leads to a higher cooling rate as less superheat to be extracted from the mould and the melt. The low pouring temperature, which was used in this experimental work, developed small grain size diameter and more globular microstructure as the low pouring temperature helps to increase the cooling rate. The microstructure which was executed with the pouring temperature of 645 °C produced smaller diameter size and more spherical primary grain structure than the pouring temperature of 685 °C. The average primary grain diameter and circularity were used to determine the size and shape of the microstructure to support this finding. The average primary grain diameter of sample 2 was higher while circularity was lower than sample 8. Sample 8 produced by the lower pouring temperature, which was executed at pouring temperature of 645 °C. The higher pouring temperature leads to the slower cooling rate as more time needed by the systems to extract the heat from the above to below the liquidus temperature.

Lower pouring temperature produced smaller grain structure can be explained by the fact that the formation of microstructure merely depended on cooling rate which was used for material processing [32–34]. The cooling rate affects the formation of microstructure by the magnitude of undercooling temperature during solidification [35]. The undercooling is the difference between the equilibrium transformation temperature and temperature, which the material cools before the start of the phase transformation.

The undercooling is influenced by the solidification rates, which are influenced by the type of a mould material, mould thickness and similar. Therefore, the formation of a microstructure which evolves within material depends on the degree of undercooling. The undercooling becomes larger when the cooling rate is higher. The increment in undercooling increases the amount of nucleation, which is ultimately resulting in a smaller grain size. During the solidification process, as the undercooling temperature and time increase, the melt potential nucleation decreases resulting in a coarse-grained structure deformation. The higher cooling rate is therefore associated with a smaller grain size and a globular microstructure.

Cooling rate determines the success of DTM to produce smaller primary phase structure and spheroidal microstructure [34,36,37]. The principle of DTM which allows for a quick heat change retards the formation of a microstructure. The chilling effect which occurs within the copper mould produced smaller nuclei and affected the formation of a spheroidal microstructure. The results in DTM suggest that all the samples except sample 10 were suitable for thixoforming operation.

The suitable thixoforming feedstock primary grain structure was found in the range of approximately 100 μm [26].

4.2 Effect of Holding Time

The role of holding time in DTM was to ensure an adequate fraction solid before quenching. The formation of a smaller size and a globular microstructure by using DTM was influenced by fraction solid volume in molten metal before quenching [38–40]. This fraction solid was estimated by determining the temperature drops during the holding period. Based on separated experimental works, the temperature inside DTM moulds during holding time was dropped at 0.7 °C/s. The different fraction solids used in this experimental work show the apparent changes in microstructure evolution. The formation of smallest average primary grain diameter in the DTM experimental work occurred at pouring temperature of 685 °C and holding time of 20 s (see Fig. 3 (a)). The sample was quenched at the temperature of 671 °C which it was in fully liquid state condition.

The observed correlation between holding time and fraction solid might be explained in this way, during rapid solidification after molten alloy was poured into a copper mould, the nuclei was started to deform from the liquid condition. The nuclei were evolved and impinged to each other within the material and later produced a dendritic microstructure as in typical solidification process. During this process (from the liquid to dendritic microstructure formation), the fraction solid which occurred in the material was increased as it approached the solidus temperature. The formation of the nuclei which was small at this stage, become larger due to the increment of fraction solid volume. The quenching technique which was performed before nuclei become larger captured a smaller and finer globular shape microstructure.

Sample 3 was quenched into ambient temperature water while it still in fully liquid condition (temperature at 671 °C). The quenching action had provided chilling environment when copper mould and molten alloy reached water. This chilling action allows rapid solidification of the melt that later catalysed nuclei formation and produced a large number of small size structures. Proper selection of a holding time in DTM is crucial to allow the formation of a desired microstructure feature due to fraction solid effect. Results in this experimental work show the fraction solid has influenced a microstructure formation. The fraction solid is one of important parameters in SSM, which determines material flowability, similar like in conventional casting process. A different fraction solid which was used in this experimental work has showed the apparent changes in microstructure evolution.

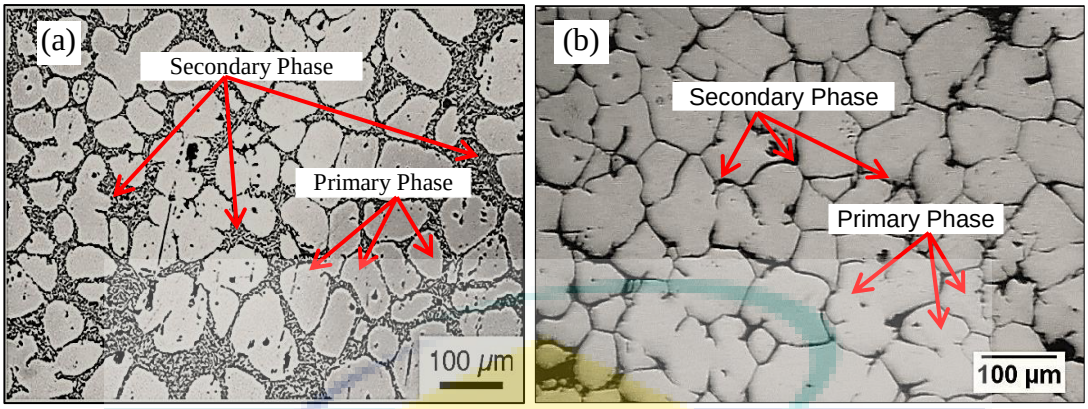

Fig. 13. Microstructure formation for two different raw materials which processed by using DTM with (a) aluminium A356 [41] and (b) aluminium 7075 (this work).

The formation of a globular microstructure in DTM was typically influenced by the raw material used. In order to show this, a comparison was made between aluminium A356 and 7075 which processed by using a DTM [41]. The microstructure for A356 from the literature and 7075 from this work are presented in Fig. 13. Both samples were processed at nearly similar pouring temperature in the range of 640 to 645 °C and holding time in the range of 40 to 75 s. The A356 microstructure was slightly more globular than 7075 with obvious distinction for the primary and secondary phase formation. Even though some of the research indicated that there was likely to process 7075 in semi-solid range temperature, but with this experimental work results, the A356 DTM feedstock billets showed more superior than 7075 in the scope of globular microstructure and the distinction between primary and secondary phase. Furthermore, it was also found that in the case of casting alloy 7075, the eutectic phase and globular structure were less to appear than for the casting alloy A356 [42].

4.3 EDXS Analysis

The EDXS results revealed compositions for primary phase (α-Al) for DTM samples consist with Al, Zn and Mg such as in Table 2. Further analysis was made at the grain boundary area or secondary (liquid) phase. The grain boundary compositions for the DTM specimen were contained only with Al and Cu as shown in Table 3. The difference in composition at the grain boundary for both specimens was likely because of the precipitation sequence. The solidification process for the DTM was unable to provide a complete precipitation sequence because the samples were quenched into ambient temperature water. The precipitation sequence of Aluminium 7075 was started with α-Al, followed by the Al + Al_3Fe and then Al + Mg_2Si. The next reaction was the eutectic phase, which precipitates last during solidification and melt first during heating consist of Al + Al_2Cu + $MgZn_2$ + $Al_2Mg_3Zn_3$. The eutectic phase occurred between the primary phases (α-Al) at the grain boundaries [26,28]. This phenomenon explained the cause of different compositions at the grain boundary which allowed only Al and

Cu elements within the DTM sample as a complete precipitation sequence not occurred.

4. Conclusion

The combination of an adequate pouring temperature and a holding time produced and appropriate smaller size and a globular microstructure. In particular, the cooling rate and the fraction solid volume also play the important roles in determining the formation of a spheroidal microstructure and finer structure. The wrought aluminium 7075 which tend to have a narrow temperature window and high flowability resistance used in this research produced average primary microstructure phase diameter in the range of 82 to 123 µm and circularity in the range of 0.55 to 0.67. Higher pouring temperature was found significantly produced higher secondary phase that led to greater fluidity within sample. The higher cooling rate that was used for SSM feedstock processing has produced a small, globular and a uniform microstructure. The combination of pouring temperature at 685 °C and the holding time of 20 seconds produced the smallest primary phase structure size. Likewise, the combination between pouring temperature and holding time of 665 °C and 60 s respectively produced the highest circularity value at 0.5 fs. The finding presented in this research contribute details understanding and information regarding the behaviours of the wrought aluminium 7075 processed by DTM for thixoforming.

Acknowledgements

The authors would also like to acknowledge the support from Universiti Malaysia Pahang (RDU151412) for funding this work.

References

[1] Z. Fan, Semisolid metal processing, Int. Mater. Rev. 47 (2002) 1–37. doi:10.2464/jilm.45.346.

[2] H. V. Atkinson, Modelling the semisolid processing of metallic alloys, Prog. Mater. Sci. 50 (2005) 341–412. doi:10.1016/j.pmatsci.2004.04.003.

[3] M.C. Flemings, Behavior of Metal Alloys in the Semisolid State, Metall. Trans. A. 22A (1991) 957–981.

[4] D.H. Kirkwood, C.M. Sellars, L.G. Boyed, Thixotropic materials, 5133811, 1992. doi:10.1145/634067.634234.

[5] O. Lashkari, R. Ghomashchi, The implication of rheology in semi-solid metal processes: An overview, J. Mater. Process. Technol. 182 (2007) 229–240. doi:10.1016/j.jmatprotec.2006.08.003.

[6] D.B. Spencer, R. Mehrabian, M.C. Flemings, Rheological behavior of Sn-15 pct Pb in the crystallization range, Metall. Trans. 3 (1972) 1925–1932. doi:10.1007/BF02642580.

[7] D. Brabazon, D.J. Browne, A.J. Carr, Mechanical stir casting of aluminium alloys from the mushy state: Process, microstructure and mechanical

properties, Mater. Sci. Eng. A. 326 (2002) 370–381. doi:10.1016/S0921-5093(01)01832-9.

[8] V. Suri, K.-O. Yu, Defects formation, in: K.-O. Yu (Ed.), Model. Cast. Solidif. Process., CRC Press, New York, 2002: pp. 95–122.
[9] A. Rassili, H. V. Atkinson, A review on steel thixoforming, Trans. Nonferrous Met. Soc. China (English Ed. 20 (2010) s1048–s1054. doi:10.1016/S1003-6326(10)60629-2.
[10] J. Shin, T. Kim, D.E. Kim, D. Kim, K. Kim, Castability and mechanical properties of new 7xxx aluminum alloys for automotive chassis/body applications, J. Alloys Compd. 698 (2017) 577–590. doi:10.1016/j.jallcom.2016.12.269.
[11] Y. Birol, Semi-solid processing of the primary aluminium die casting alloy A365, J. Alloys Compd. 473 (2009) 133–138. doi:10.1016/j.jallcom.2008.05.074.
[12] M. Bünck, N. Warnken, A. Bührig-Polaczek, Microstructure evolution of rheo-cast A356 aluminium alloy in consideration of different cooling conditions by means of the cooling channel process, J. Mater. Process. Technol. 210 (2010) 624–630. doi:10.1016/j.jmatprotec.2009.11.011.
[13] A. Abedi, M. Shahmiri, B. Amir Esgandari, B. Nami*, Microstructural evolution during partial remelting of Al–Si alloys containing different amounts of magnesium, J. Mater. Sci. Technol. 29 (2013) 971–978. doi:10.1016/j.jmst.2013.04.021.
[14] L. Chen, Y. Zhao, F. Yan, H. Hou, Statistical investigations of serpentine channel pouring process parameters on semi-solid ZL101 aluminum alloy slurry using response surface methodology, J. Alloys Compd. 725 (2017) 673–683. doi:10.1016/j.jallcom.2017.07.169.
[15] M.J. Hussey, A direct thermal method of attaining globular morphology in the primary phase of alloys, in: Proc. 7th Int. Conf. Semi-Solid Process. Alloy. Compos. (S2P ’02), Tsukuba, 2002: pp. 575–580.
[16] A.H. Ahmad, S. Naher, D. Brabazon, Effects of direct thermal method temperature and time on A356 microstructure, in: 15Th Int. Conf. Adv. Mater. Process. Technol., Wollongong, 2012.
[17] L. Zhang, W. Li, J.P. Yao, Microstructures and thermal stability of the semi-solid 2024 aluminum alloy prepared using the pulsed magnetic field process: Effects of technological parameters, J. Alloys Compd. 554 (2013) 156–161. doi:10.1016/j.jallcom.2012.10.185.
[18] L. Yageng, M. Weimin, Z. Wenzhi, Y. Bin, Rheological behavior of semi-solid 7075 aluminum alloy at steady state, China Foundry. 11 (2014) 79–84.
[19] G. Chen, F. Lin, S. Yao, F. Han, B. Wei, Y. Zhang, Constitutive behavior of aluminum alloy in a wide temperature range from warm to semi-solid regions, J. Alloys Compd. 674 (2016) 26–36. doi:10.1016/j.jallcom.2016.02.254.
[20] X.Z. Zhang, T.J. Chen, Y.S. Chen, Y.J. Wang, H. Qin, Effects of solution treatment on microstructure and mechanical properties of powder thixoforming 6061 aluminum alloy, Mater. Sci. Eng. A. 662 (2016) 214–226. doi:10.1016/j.msea.2016.03.060.
[21] J. Jiang, H. V. Atkinson, Y. Wang, Microstructure and Mechanical Properties of 7005 Aluminum Alloy Components Formed by Thixoforming, J. Mater. Sci. Technol. 33 (2017) 379–388. doi:10.1016/j.jmst.2016.07.014.

[22] X.H. Chen, H. Yan, Constitutive behavior of Al2O3np/Al7075 composites with a high solid fraction for thixoforming, J. Alloys Compd. 708 (2017) 751–762. doi:10.1016/j.jallcom.2017.03.063.

[23] S. Chayong, H. V. Atkinson, P. Kapranos, Thixoforming 7075 aluminium alloys, Mater. Sci. Eng. A. 390 (2005) 3–12. doi:10.1016/j.msea.2004.05.004.

[24] D. Liu, H. V. Atkinson, P. Kapranos, W. Jirattiticharoean, H. Jones, Microstructural evolution and tensile mechanical properties of thixoformed high performance aluminium alloys, Mater. Sci. Eng. A. 361 (2003) 213–224. doi:10.1016/S0921-5093(03)00528-8.

[25] G. Vaneetveld, A. Rassili, J.C. Pierret, J. Lecomte-Beckers, Improvement in Thixoforging of 7075 Aluminium Alloys at High Solid Fraction, Solid State Phenom. 141–143 (2008) 707–712. doi:10.4028/www.scientific.net/SSP.141-143.707.

[26] H. V. Atkinson, K. Burke, G. Vaneetveld, Recrystallisation in the Semi-Solid State in 7075 Aluminium Alloy, Mater. Sci. Eng. A. 490 (2008) 266–276. doi:10.1007/s12289-008-0220-z.

[27] D.I. Jang, Y.O. Yoon, S.K. Kim, Thixoextrusion for 7075 Al Wrought Alloy Tube, Semi-Solid Process. Alloy. Compos. X. 141–143 (2008) 267–270\r798. doi:10.4028/www.scientific.net/SSP.141-143.267.

[28] L. Bäckerud, G. Chai, J. Tamminen, Solidification characteristics of aluminium alloys (Vol. 2: Foundry Alloys.), University of Stockholm, Stockholm, 1991.

[29] ASM International, ASM Handbook Volume 9 : Metallography and Microstructures, ASM International, Materials Park, OH, 2004. doi:10.1016/S0026-0576(03)90166-8.

[30] A.H. Ahmad, S. Naher, D. Brabazon, Effects of Cooling Rates on Thermal Profiles and Microstructure of Aluminium 7075, Int. J. Automot. Mech. Eng. 9 (2014) 1685–1694.

[31] A.H. Ahmad, S. Naher, D. Brabazon, The Effect of Direct Thermal Method, Temperature and Time on Microstructure of a Cast Aluminum Alloy, Mater. Manuf. Process. 29 (2014) 134–139. doi:10.1080/10426914.2013.822980.

[32] G. Gonzalez, G.A. Lara-Rodriguez, A. Sandoval-Jiménez, W. Saikaly, A. Charai, The influence of cooling rate on the microstructure of an Al-Ni hypereutectic alloy, Mater. Charact. 59 (2008) 1607–1612. doi:10.1016/j.matchar.2008.02.006.

[33] M. Mukherjee, U. Ramamurty, F. Garcia-Moreno, J. Banhart, The effect of cooling rate on the structure and properties of closed-cell aluminium foams, Acta Mater. 58 (2010) 5031–5042. doi:10.1016/j.actamat.2010.05.039.

[34] G.M. Zeer, M. V. Pervukhin, E.G. Zelenkova, Effect of cooling rate on microstructure formation during crystallization of aluminum alloy 1417M, Met. Sci. Heat Treat. 53 (2011) 210–212. doi:10.1007/s11041-011-9370-6.

[35] S. Gowri, F.H. Samuel, Effect of cooling rate on the solidification behavior of Al-7 Pct Si-SiCp metal-matrix composites, Metall. Trans. A. 23 (1992) 3369–3376. doi:10.1007/BF02663446.

[36] V.A. Hosseini, S.G. Shabestari, R. Gholizadeh, Study on the effect of cooling rate on the solidification parameters, microstructure, and mechanical properties of LM13 alloy using cooling curve thermal analysis technique, Mater. Des. 50 (2013) 7–14. doi:10.1016/j.matdes.2013.02.088.

[37] L.. Dobrzañski, R. Maniara, J.. . Sokolowski, The effect of cooling rate on microstructure and mechanical properties of AC AlSi9Cu alloy, Arch. Mater. Sci. Eng. 28 (2007) 105–112. doi:10.1155/2013/826758.
[38] T. Haga, P. Kapranos, Simple rheocasting processes, J. Mater. Process. Technol. 130–131 (2002) 594–598. doi:10.1016/S0924-0136(02)00819-1.
[39] S.J. Satya, V. Kumar, N.S. Barekar, K. Biswas, B.K. Dhindaw, Microstructural evolution under low shear rates during rheo processing of LM25 alloy, J. Mater. Eng. Perform. 21 (2012) 2283–2289. doi:10.1007/s11665-012-0166-7.
[40] M. Reisi, B. Niroumand, Initial stages of solidification during semisolid processing of a transparent model material, Mater. Chem. Phys. 135 (2012) 738–748. doi:10.1016/j.matchemphys.2012.05.053.
[41] D.J. Browne, M.J. Hussey, A.J. Carr, D. Brabazon, Direct thermal method: new process for development of globular alloy microstructure, Int. J. CAST Met. Res. 16 (2003) 418–426. doi:10.1179/136404603225007854.
[42] S.W. Oh, J.W. Bae, C.G. Kang, Effect of electromagnetic stirring conditions on grain size characteristic of wrought aluminum for rheo-forging, J. Mater. Eng. Perform. 17 (2008) 57–63. doi:10.1007/s11665-007-9150-z.

CHAPTER 4

CONCLUSION

The thermal analysis with different cooling rates was successfully investigated. The difference in cooling rate conditions has a significant effect to the changes of phases during solidification process. The liquidus, eutectic, and solidus temperature for a normal cooling rate (2.23 °C/s) occurred at 619.30 °C, 438.48 °C, and 421.90 °C whilst for intermediate cooling rate (2.88 °C/s) occurred at 603.84 °C, 415.0 °C, and 393.93 °C, respectively. The liquidus, eutectic, and solidus temperature for a high cooling rate (3.20 °C/s) were recorded at a lower temperature than the other cooling rate conditions which were at 589.91 °C, 405.55 °C, and 385.69 °C.

The combination of an adequate pouring temperature and a holding time produced and appropriate smaller size and a globular microstructure. In particular, the cooling rate and the fraction solid volume also play the important roles in determining the formation of a spheroidal microstructure and finer structure. The wrought aluminium 7075 which tend to have a narrow temperature window and high flowability resistance used in this research produced average primary microstructure phase diameter in the range of 82 to 123 µm and circularity in the range of 0.55 to 0.67. Higher pouring temperature was found significantly produced higher secondary phase that led to greater fluidity within sample. The higher cooling rate that was used for SSM feedstock processing has produced a small, globular and a uniform microstructure. The combination of pouring temperature at 685 °C and the holding time of 20 seconds produced the smallest primary phase structure size. Likewise, the combination between pouring temperature and holding time of 665 °C and 60 s respectively produced the highest circularity value at 0.5 fs. The finding presented in this research contribute details understanding and information regarding the behaviours of the wrought aluminium 7075 processed by DTM for thixoforming.